
Recent Progress in the Freeze-Etching Technique

H. Moor

Phil. Trans. R. Soc. Lond. B 1971 **261**, 121-131

doi: 10.1098/rstb.1971.0042

Email alerting service

Receive free email alerts when new articles cite this article - sign up in the box at the top right-hand corner of the article or click [here](#)

To subscribe to *Phil. Trans. R. Soc. Lond. B* go to: <http://rstb.royalsocietypublishing.org/subscriptions>

Recent progress in the freeze-etching technique

BY H. MOOR

Swiss Federal Institute of Technology, Department of Botany, Laboratory of Electron Microscopy, Universitätstrasse 2, 8006 Zürich, Switzerland

[Plates 19 to 22]

The freeze-etching technique must be improved if structures at the molecular size level are to be seen. The limitations of the technique are discussed here together with the progress made in alleviating them. The vitrification of living specimens is limited by the fact that very high freezing rates are needed. The critical freezing rate can be lowered on the one hand by the introduction of antifreeze agents, on the other hand by the application of high hydrostatic pressure. The fracture process may cause structural distortions in the fracture face of the frozen specimen. The 'double-replica' method allows one to evaluate such artefacts and provides an insight into the way that membranes split. During etching there exists the danger of contaminating the fracture faces with condensable gases. Because of specimen temperatures below $-110\text{ }^{\circ}\text{C}$, special care has to be taken in eliminating water vapour from the high vacuum. An improvement in coating freeze-etched specimens has resulted from the application of electron guns for evaporation of the highest melting-point metals. If heat transfer from gun to specimen is reduced to a minimum, Pt, Ir, Ta, W and C can be used for shadow casting. Best results are obtained with Pt–C and Ta–W. With the help of decoration effects Pt–C shadow castings give the most information about the fine structural details of the specimen.

INTRODUCTION

Freeze-etching, in the last five years, has become a routine laboratory technique. The main advantage of this method is that an image of cells stabilized in the living state is obtainable. At the molecular level, the application of freeze-etching encounters limitations which are mainly fixed by the nature of the physical treatments used. It has been our task to explore and elucidate the causes of such limitations in order to overcome them and thereby to extend the range of the method down to molecular dimensions.

Essentially, freeze-etching consists of four preparational steps: freezing, fracturing, etching and coating (Moor 1966*a*). Every individual step raises its own problems concerning technical improvements and factors which may influence the apparent structure of the object being examined.

FREEZING

The aim of freezing is to solidify a specimen in the natural state without any changes in structure and chemistry. This can only be achieved by vitrification (Moor 1964). Calculations and experiments have shown that a system containing a high amount of water can only be vitrified if the temperature interval from 0 to $-100\text{ }^{\circ}\text{C}$ is passed in less than 0.01 s (Riehle 1968). This is equivalent to a freezing rate of at least $10\,000\text{ K s}^{-1}$. Limitations arise from the fact that heat can only be extracted through the specimen surface by conduction. The low thermal conductivity of watery systems reduces the vitrified region of a specimen to a superficial zone of 2 to 3 μm in thickness, even if the heat exchange at the surface could be enlarged to an infinite value. Therefore, the vitrification of thicker objects cannot be achieved by further improvements of the freezing technique, instead the properties of the specimens have to be changed.

The critical freezing rate sufficient for vitrification can be lowered considerably. One way of doing this consists of introducing antifreeze agents (Moor 1966*a*). Experience has shown that the

critical freezing rate is lowered to a range of 100 to 10 K s⁻¹ by the action of glycerol or similar substances (ethylene glycol, dimethyl sulphoxide, pyridine *N*-oxide) in a concentration of 20 to 30 %. Impregnated specimens up to 1 mm in thickness can be vitrified very easily. But the impregnation of living cells with such agents in high concentration introduces many artefacts. Physiological changes may cause morphological alterations like a swelling of mitochondria or of the e.r. cisternae (figures 1, 2, 5 and 6, plate 19). Fine structures embedded in the

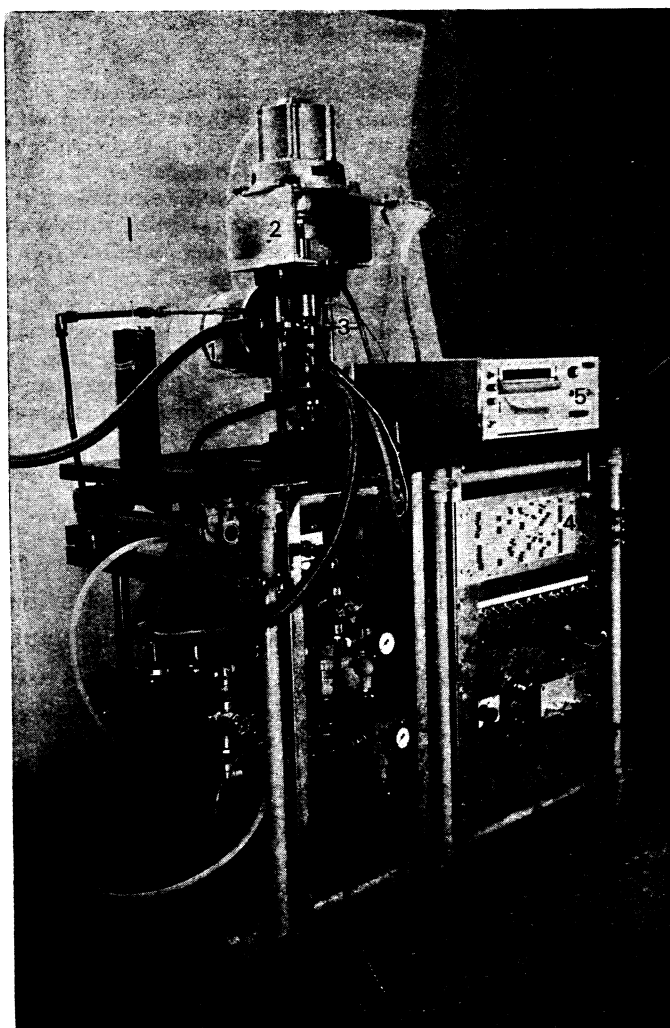


FIGURE 3. The apparatus used for snap-freezing under high pressure. 1, nitrogen supply; 2, pressure supply; 3, specimen stage; 4, time relay for automatic processing; 5, u.v. recorder of temperature and pressure in the specimen stage.

ground plasm, e.g. microtubular subunits (Moor 1967), are hidden or blurred. More drastic effects are introduced if the specimen is poisoned or cannot take up the antifreeze. A considerable reduction of osmotic influences may be achieved by the application of 'composite antifreeze agents' (Wecke 1968), which generally contain 5 % glycerol, 5 % serum globulin, 20 % of a mixture of different amino acids and trace elements and 0.25 % polyvinyl pyrrolidone. These have been successfully used with some flagellates, but the application is thus far limited to single-celled, small specimens.

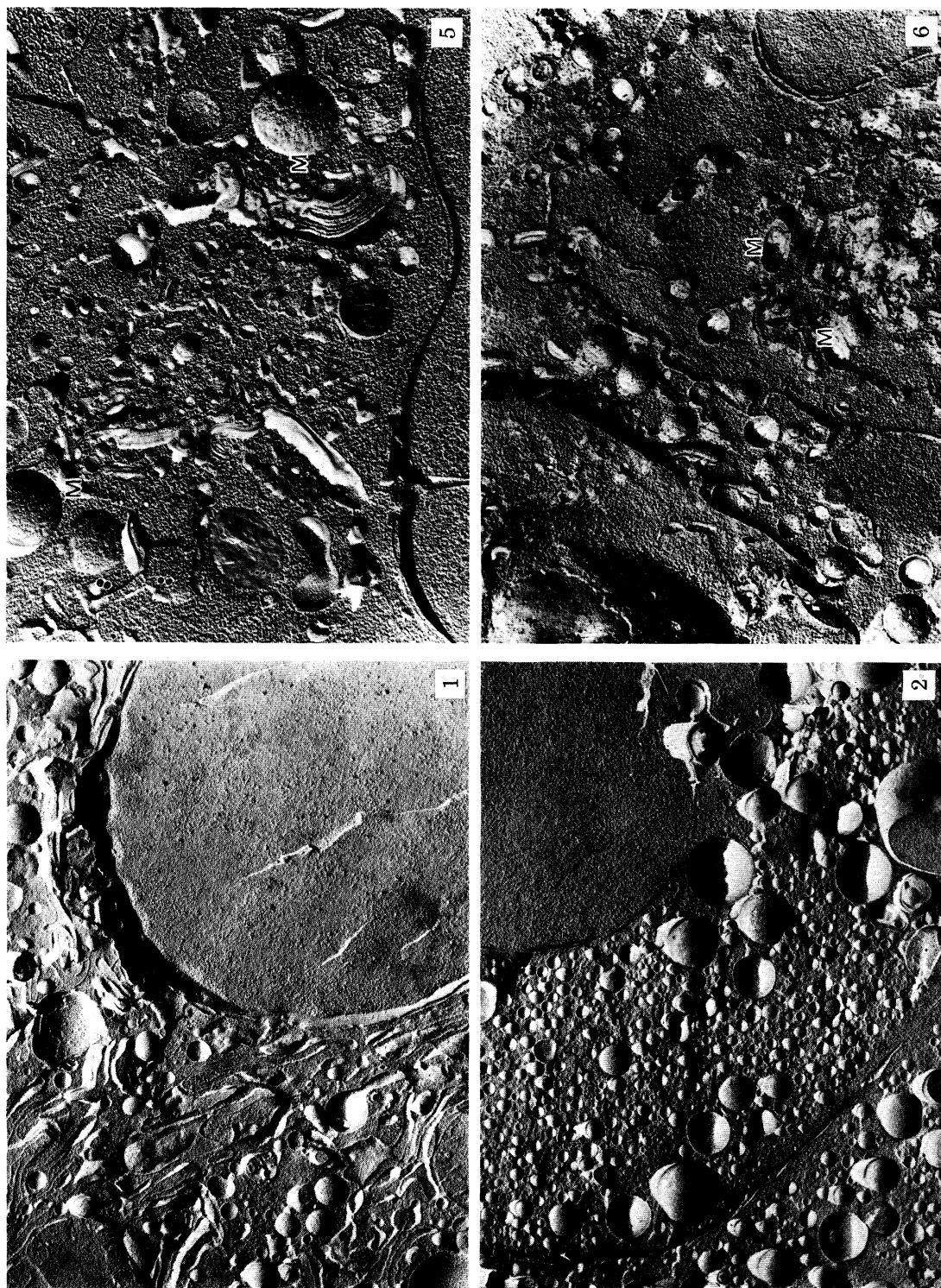
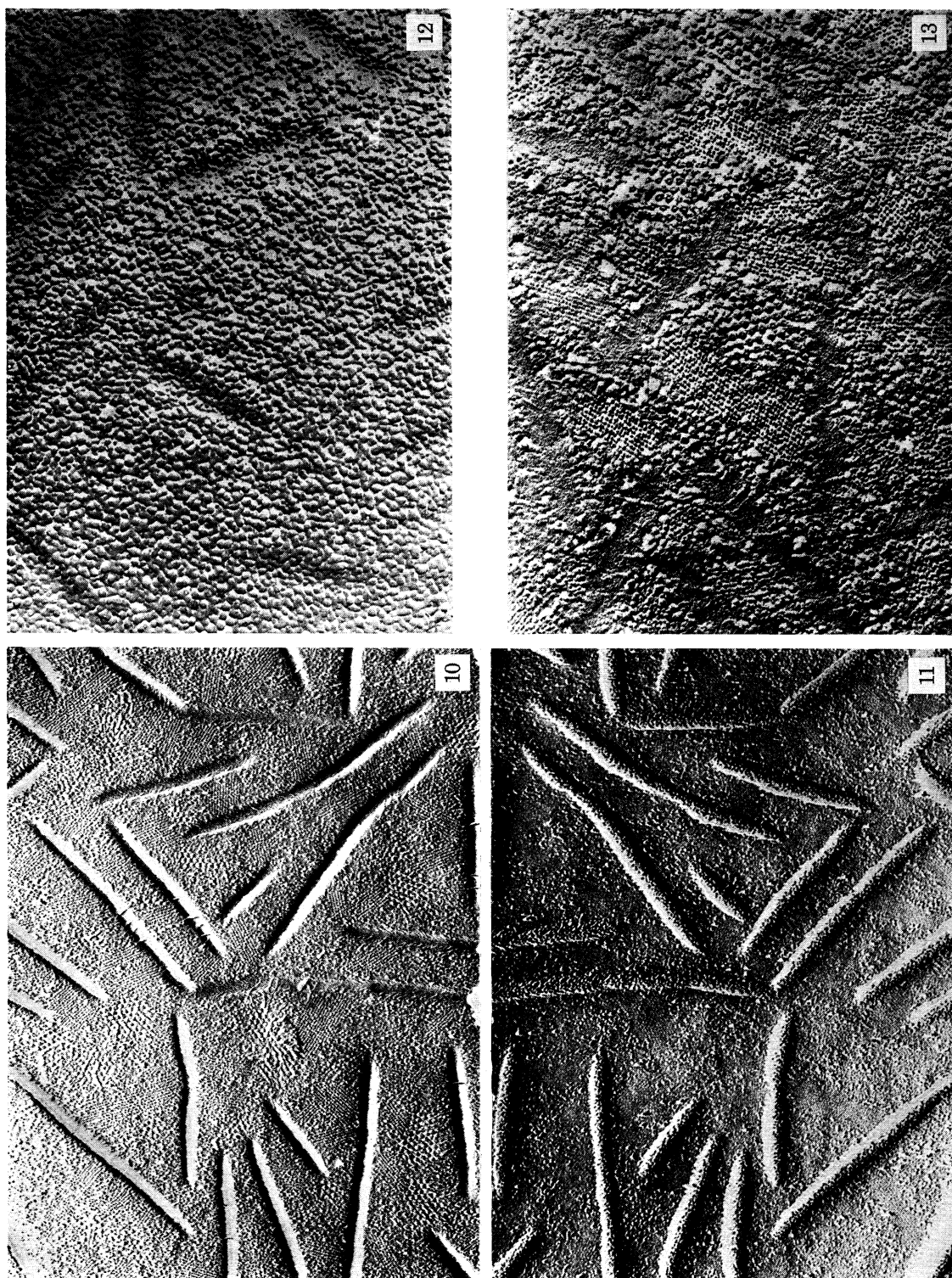


FIGURE 1. A liver cell, prefixed with glutaraldehyde, impregnated with 30% glycerol and freeze-etched, shows a laminar e.r. system. (Magn. $\times 12000$.)

FIGURE 2. The same specimen, treated with 30% glycerol in the living state exhibits a vesiculated e.r. system. (Magn. $\times 12000$.)

FIGURE 5. Part of an ascites tumour cell, protected with 30% glycerol and freeze-etched in the usual way. (Magn. $\times 19200$.)

FIGURE 6. The same type of specimen freeze-fixed under high pressure without antifreeze protection. The same quality of vitrification is obtainable with either antifreeze agents or high pressure freezing. (Magn. $\times 12800$.) The glycerol treatment produces spherical mitochondria (M), the pressure freezing rod-shaped organelles.



FIGURES 10, 11. Double replica of the plasmalemma of baker's yeast. The two complementary figures can be brought into juxtaposition by folding along the axis between the two photographs. In figure 10 we are looking from the cell wall side, in figure 11 from the cytoplasmic side at the fracture face. (Magn. $\times 48,000$.)

FIGURE 12. Heavy contamination on a yeast plasmalemma at -150°C exposed to a conventional vacuum of 10^{-4} N m^{-2} Torr). (Magn. $\times 92,000$.)

FIGURE 13. A non-contaminated yeast plasmalemma at -150°C exposed to a cleansed vacuum of 10^{-5} N m^{-2} (10^{-7} Torr). (Magn. $\times 92,000$.)

A second way of reducing the critical freezing rate consists of applying high pressure. This approach allows one to omit the introduction of any antifreeze agent. At 204.5 MN m^{-2} (2045 bar) the freezing-point of pure water is lowered to a minimum of -22°C (Bridgman

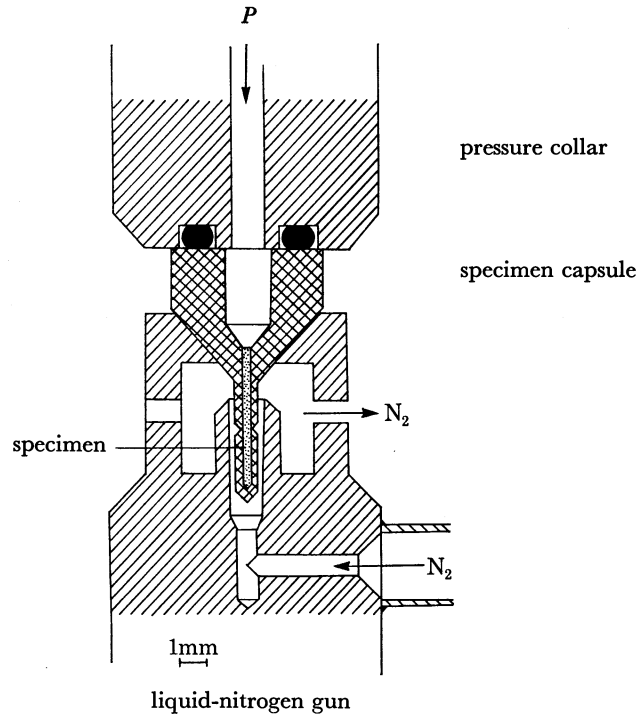


FIGURE 4. Schematic section through the specimen stage of the pressure freezing device: the specimen capsule (see dark cross hatchings) consists of a funnel-shaped part which is mounted between pressure collar and liquid nitrogen gun. The thin-walled, closed tube of the funnel, containing the specimen, extends into the liquid nitrogen jet of the gun. Pressure is applied to the specimen by means of a water column through the pressure collar. This arrangement allows the use of liquid nitrogen at atmospheric pressure while the specimen is under high hydrostatic pressure.

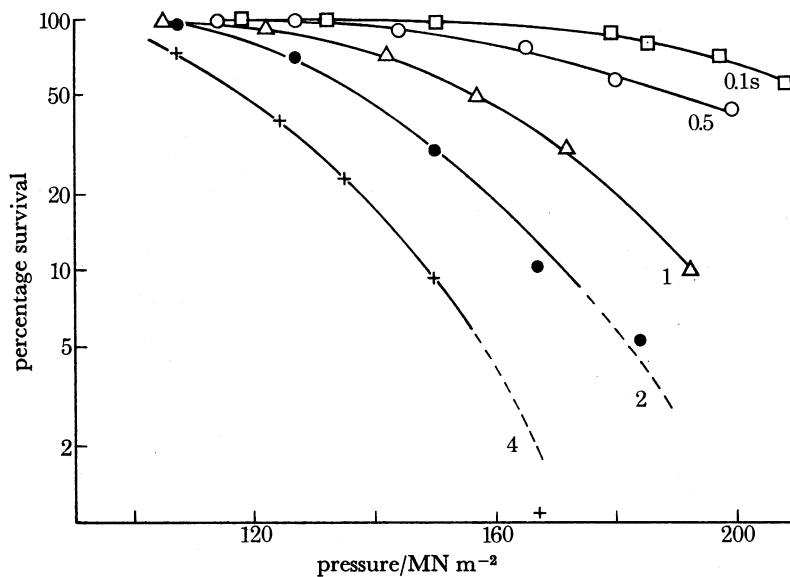


FIGURE 7. The survival rate of *Euglena* cells kept under pressure for various brief periods of time.

1912). At this pressure there is a drastic reduction in the rate of nucleation and ice crystal growth (Riehle 1968). As a result, the critical freezing rate is lowered to about 100 K s^{-1} allowing the vitrification of specimens having a thickness of 0.2 to 0.3 mm.

In an especially designed apparatus, liquid nitrogen is sprayed onto the specimen at a speed of 25 m s^{-1} (figure 3). To prevent damage to the object, it is placed in a thin-walled metal tube and exposed under pressure to the action of the cryogen (figure 4). After freezing, the metal tube containing the frozen specimen is broken at a predetermined zone. The resulting fracture face through the specimen is freeze-etched (Moor & Riehle 1968).

The disadvantage of this method is the lethal effect of high pressure. Experiments have demonstrated that cells are able to tolerate a certain pressure dose (Höchli 1969). *Euglena gracilis* cells (sensitive to the action of pressure as well as to antifreeze agents) have been subjected to different amounts of pressure for different periods of time. The determination of survival rates after such treatment indicates that the briefer the pressure time is, the higher the amount of pressure that can be tolerated (figure 7). At 200 MN m^{-2} (2000 bar) this pressure time is less than 0.1 s. In an apparatus which is now under construction the period of change from normal conditions to high pressure and vitrification is of the order of 0.01 s. It will allow more than 90 % of sensitive cells to be vitrified without lethal changes using a pressure of 200 MN m^{-2} .

The two different ways to overcome the problem of the critical freezing rate will make possible an evaluation of the artefacts involved in vitrification. The pressure-freezing itself will open new possibilities in the application of freeze-etching.

FRACTURING

The fracturing process exposes the inner surfaces of the specimen. Two aspects of this process are considered here: (1) structural changes produced by rupturing the frozen specimen, and (2) the accurate determination of the course of the fracture plane.

Insight into the extent of artefacts caused by fracturing (as well as by etching and coating) is gained by the use of the so-called 'double-replica method' (Steere & Moseley 1969, Wehrli Mühlethaler & Moor 1970). A specimen is broken along a single fracture plane creating two complementary fracture faces, both of which have to be replicated. A structural comparison of complementary places in the two replicas allows one to evaluate the occurrence of distortions and other alterations.

A special specimen holder (figure 9) adapted to a Balzers unit has been developed which allows us to process three samples simultaneously. The specimen (suspensions of cells, isolated organelles or membranes) is sandwiched between two gold disks conventionally used as object carriers (figure 8). In addition, two gold London finder grids, which are kept in alignment with a small amount of Vaseline, are placed between the disks. Then, the whole sandwich is snap-frozen and inserted into the slits of the precooled specimen holder. Fracturing under vacuum is achieved by pulling the pin, attached to the movable part of the specimen holder, with the microtome arm. This part of the holder is completely turned over and brings the two fracture faces into the right position for replication. The specimen fractures between the two finder grids, both of which support a replica during the following cleaning procedures. The identified squares of the finder grids facilitate the location of matching fracture faces.

A prominent problem, raised by the freeze-etching technique, is the description and explanation of membrane structures. Experience has demonstrated that the fracture faces of several

membrane systems show two rather different structural aspects. On the convex face of the plasmalemma of baker's yeast for example one finds relatively large particles arranged in a characteristic manner and filaments which may cross the invaginations (figure 10, plate 20). On the complementary concave face the negative of these structures cannot be detected

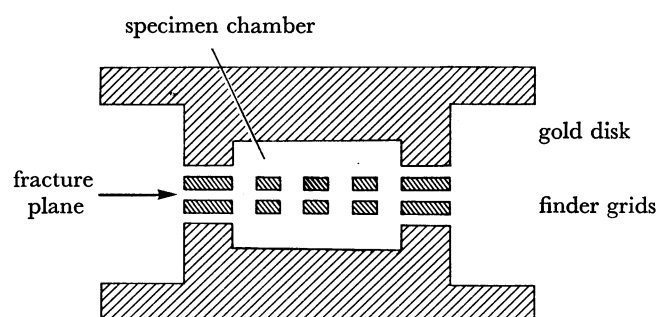


FIGURE 8. The elements of the 'sandwich' used for the production of double replicas.

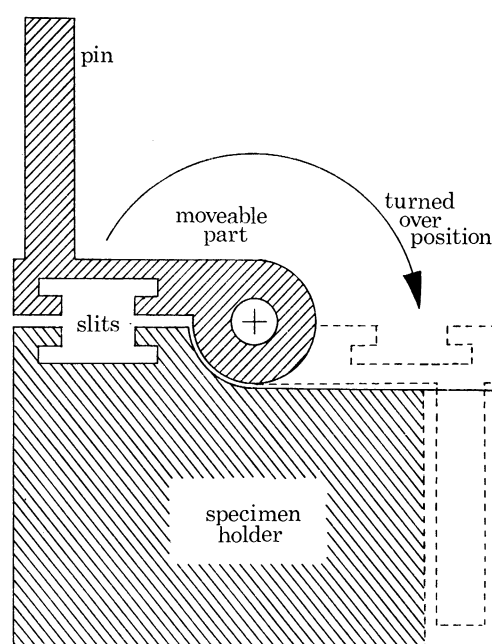


FIGURE 9. The specimen holder for double replication: the sandwiched specimen is inserted into the slits and fractured by turning over the moveable part.

(figure 11, plate 20). The fact that these two aspects do not behave like positive and negative in detail led us to the conclusion that there should exist two different fracture planes per membrane following its inner and outer surface (Moor 1966*b*). The double-replica method shows that membranes split along one plane. However, the two exposed fracture faces do not fit together in detail. One reason might be the occurrence of distortions during the fracturing procedure. The discussion to follow will show that additional artefacts may also expand this structural gap between positive and negative.

Concerning the accurate course of the fracture plane, the described technique indicates that main membrane constituents are separated by fracturing (Wehrli, Mühlethaler & Moor 1970). The general assumption is that a membrane has a central layer with inserted or apposed

functional centres. The results of the double-replica method do not tell one whether the fracture plane follows either one or the other side of this central layer or splits it into two parts.

Deep etching, which means the revealing of frozen membranes by sublimation alone, should result in real surface views of membranes. Pinto & Branton (1970) have shown that ferritin particles, covalently bound to the surface of the ghosts of erythrocytes, can only be demonstrated after deep etching. However, the properties of this membrane may be heavily altered by the influences of the isolation and coupling procedures and by the final suspension in distilled water which is necessary for deep etching. Under these conditions an artificial coat may be produced on the membrane surfaces. Therefore, it is conceivable that the fracture plane could either split a membrane into two halves or separate marker particles and other apposed materials from the central layer.

Weinstein (1969) freeze-fractured and coated tissue, and then thawed, fixed, embedded and thin-sectioned it. The replica served as marker of the fracture plane. He observed that plasma-membrane as well as e.r. cisternae (from which the ribosomes were split off) showed an intact unit-membrane structure at the fracture face. However, alterations at the fracture face during thawing and fixation cannot be excluded in principle.

The problem of how membranes split, if indeed all membranes split in the same way, is being approached with vigour from several points of view. However, no unequivocal proof of uniformity of splitting has been devised up to the present time.

ETCHING

During the time between fracturing and coating there exists the danger of contaminating the fracture face with condensable gases present in the vacuum chamber. Our experience indicates that even during the etching process this danger of artefact introduction is not excluded.

Processing a frozen specimen at -100°C in a conventional vacuum system (10^{-3} to 10^{-4} N m^{-2} ; 10^{-5} to 10^{-6} Torr) results in a reproducible portrayal of the object. Yet, from one experiment to the next, one may observe slight differences in the size of some fine structures, e.g. of the particles on membranes. This phenomenon is reinforced by the use of a specimen temperature below -110°C . A gradual lowering of the temperature results in a 'growth' of the fine structures and ends up with their disappearance under a heavy 'coat' (figure 12, plate 20). An improvement of the vacuum conditions by addition of a liquid nitrogen cooled baffle over the diffusion pump and a large cold trap in the bell jar completely eliminates these phenomena (figure 13).

A similar experience has been encountered in freeze-etching pure ice at -100°C . Conventionally an etched ice surface is covered with 'warts' which resemble certain particles observed on membranes (figures 14 and 15, plate 21). An improvement of the vacuum in the manner already described greatly reduces the number and size of these warts (figure 15). These structures can be nearly completely removed by using a titanium-sublimation pump, viton seals and a bell jar which can be baked out (figure 16, plate 21). The vacuum obtained in this way is of the order 10^{-6} N m^{-2} (10^{-8} Torr) (figure 17).

Since vacuum improvements reduce 'warts' and 'coat', it is assumed that these are produced by the condensation of residual vapours, in the vacuum chamber, onto the cold specimen surface. The effects of changes in the vacuum system mentioned above and the observation of an oriented deposition of the condensate on the ice (figure 15) suggests that this contamination

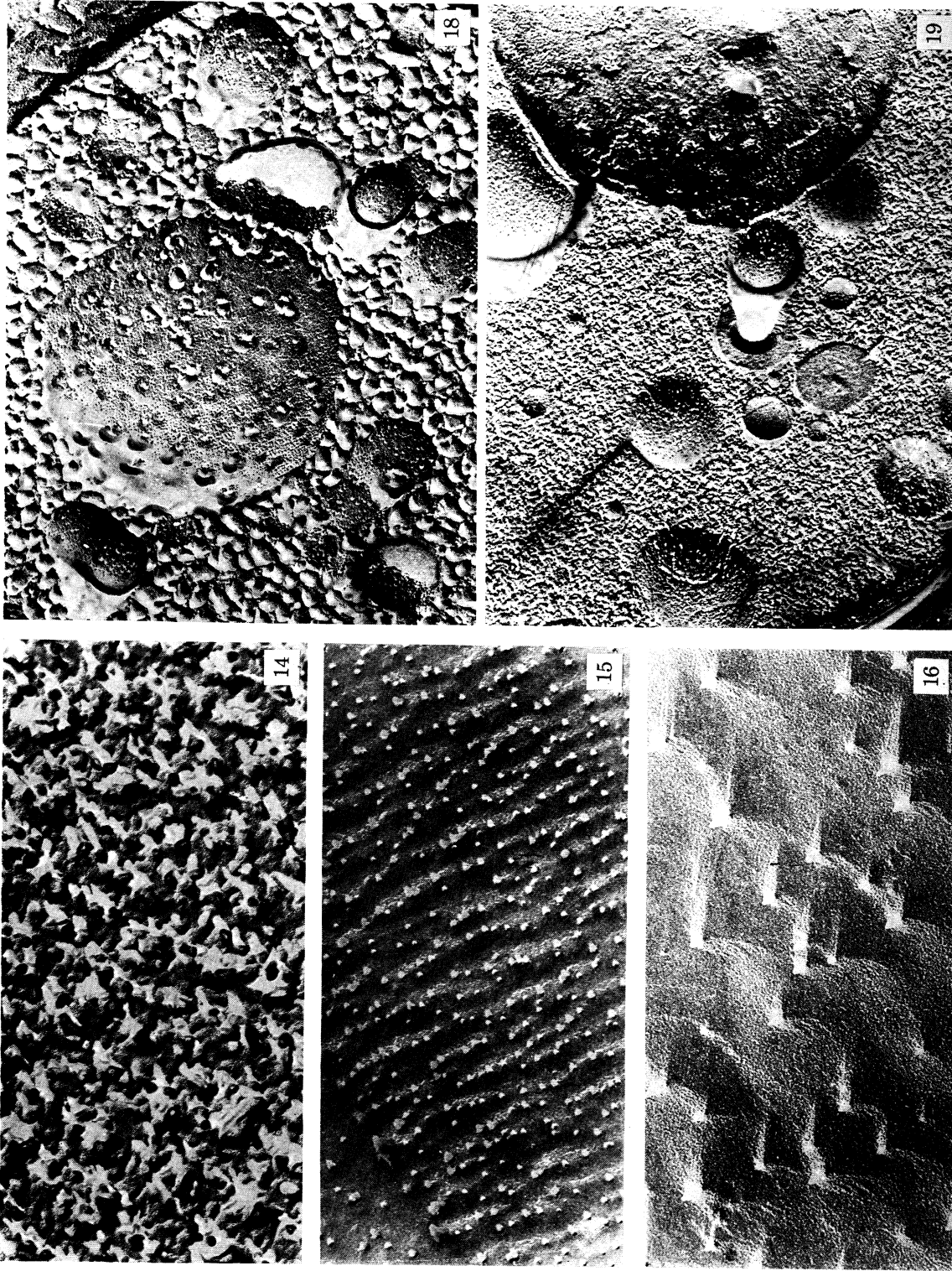


FIGURE 14. An etched ice surface at -100°C exposed to a conventional vacuum of 10^{-4} N m^{-2} (10^{-6} Torr). (Magn. $\times 48000$.)

FIGURE 15. The same specimen exposed to a cleaned vacuum of 10^{-5} N m^{-2} (10^{-7} Torr). (Magn. $\times 48000$.)

FIGURE 16. The same specimen exposed to an ultrahigh vacuum of 10^{-8} N m^{-2} (10^{-8} Torr). (Magn. $\times 56000$.)

FIGURE 18. Freeze-etched cell of baker's yeast destroyed by heat radiation. (Magn. $\times 32000$.)

FIGURE 19. An area of the same specimen without destruction. (Magn. $\times 32000$.)

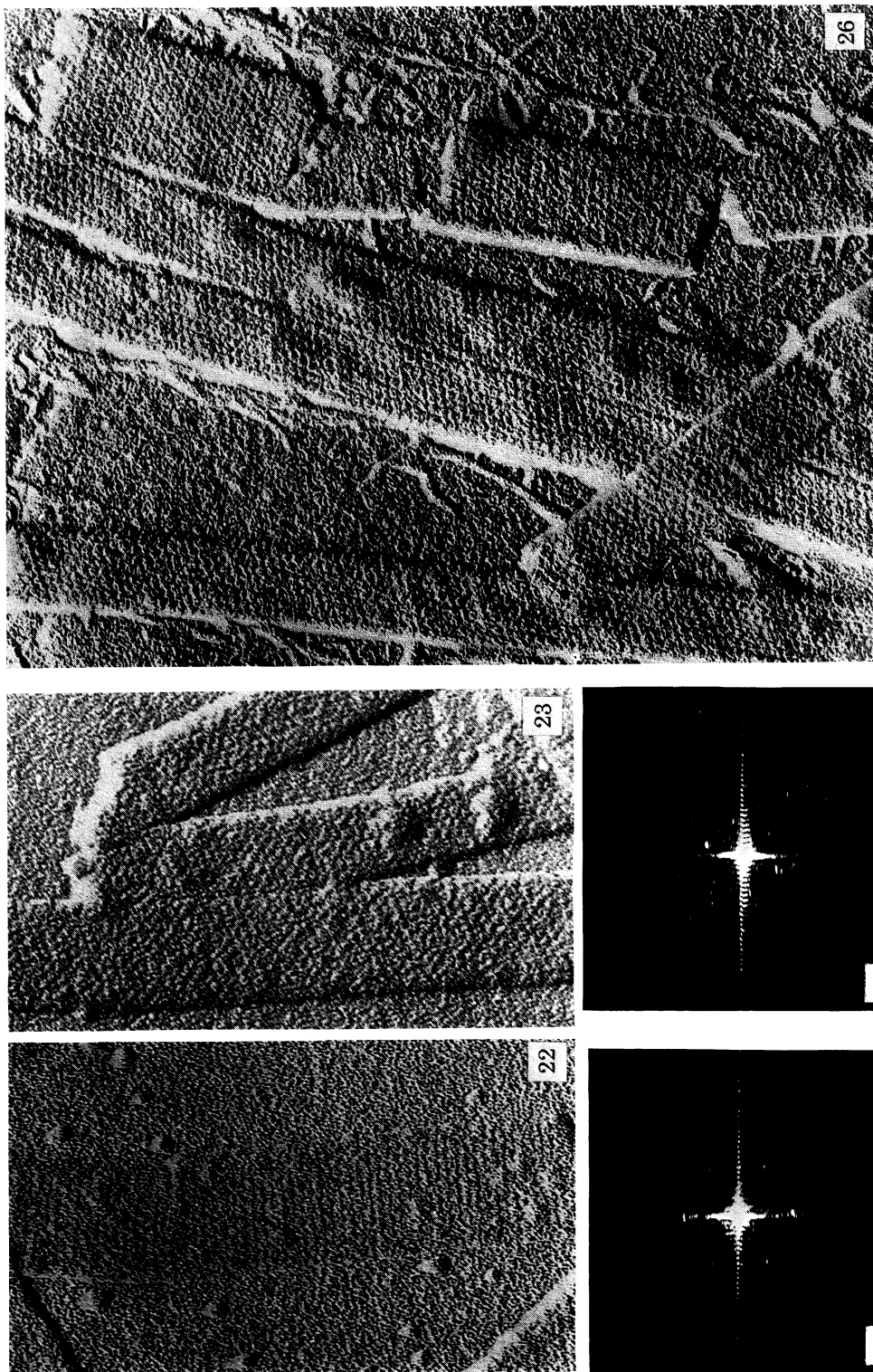


FIGURE 22. Polyhead preparation at 20 °C shadowed with Pt-C. Substructures of the capsomeres can be made visible only by optical diffraction. (Magn. $\times 132000$.)

FIGURE 23. Polyhead preparation at 20 °C shadowed with Ta-W. Substructures of the capsomeres are not visible. (Magn. $\times 132000$.)

FIGURE 24. Optical diffraction of figure 22.

FIGURE 25. Optical diffraction of figure 23.

FIGURE 26. Polyhead preparation at -150 °C shadowed with Pt-C. Substructures of the capsomeres are directly visible. (Magn. $\times 132000$.)

consists of water. The results reported demonstrate that the condensation of water depends not only on vacuum conditions and specimen temperatures but also on specimen properties. At $-100\text{ }^{\circ}\text{C}$ cellular structures may be free of contamination while the surface of ice is covered with the 'warts'.

In a conventional vacuum (10^{-4} N m^{-2} (10^{-6} Torr) in a Balzers unit) the conditions during the period of etching alter drastically if the specimen temperature is shifted from -100 to $-120\text{ }^{\circ}\text{C}$. The saturation vapour pressure of water at the specimen surface changes from 10^{-3} to

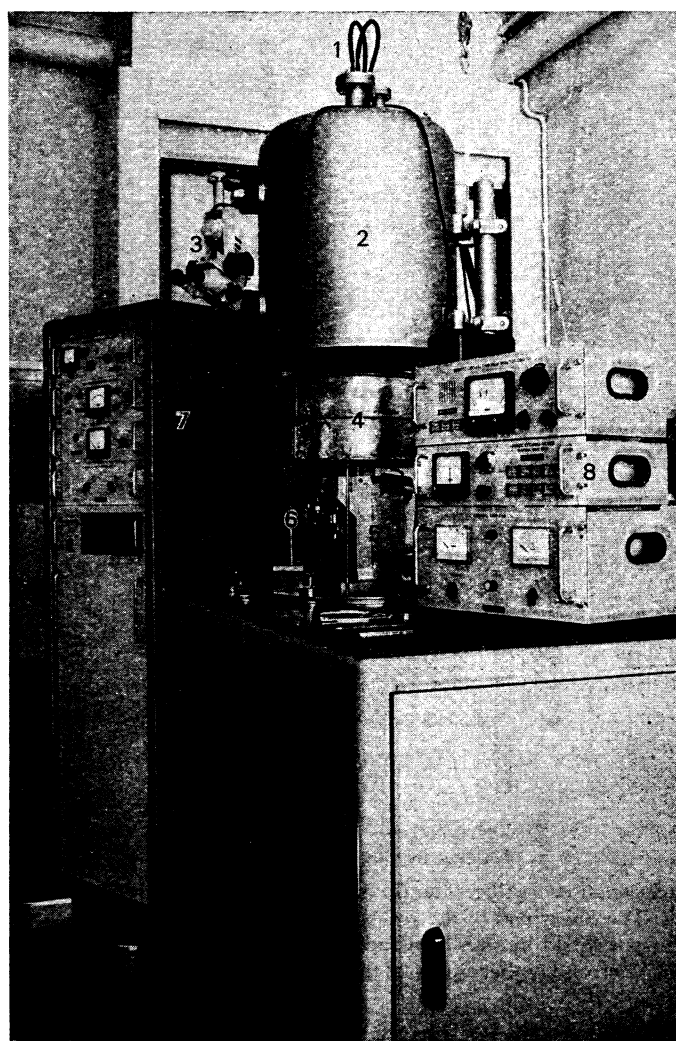


FIGURE 17. The Balzers high vacuum plant BA 510 A used for freeze-etching: 1, Ti-sublimation pump; 2, bell jar; 3, binocular microscope for specimen observation; 4, the additional large cold trap; 5, microtome; 6, electron guns, 7, vacuum control units, 8, control units for thin film measurement, freeze-etching and evaporations.

10^{-5} N m^{-2} (10^{-5} to 10^{-7} Torr). Because the conventional vacuum of 10^{-4} N m^{-2} (10^{-6} Torr) contains a large amount of water, this temperature shift results in a change from sublimation to condensation. Therefore, the observations of Staehelin & Bertaud (1969) about a 'temperature dependence of freeze-etch images' based on such an alteration do not prove a specimen transformation in the solid state but may be explained by the phenomena described above.

Using specimen temperatures below $-110\text{ }^{\circ}\text{C}$ during freeze-etching, special care has to be taken to greatly reduce the water content of the high vacuum.

COATING

The aim of coating is to produce a detailed replica on the specimen surface which, after cleaning, can be observed in the electron microscope. The amount of inherent information depends on the properties of the heavy metal used for shadow casting and on the influence of

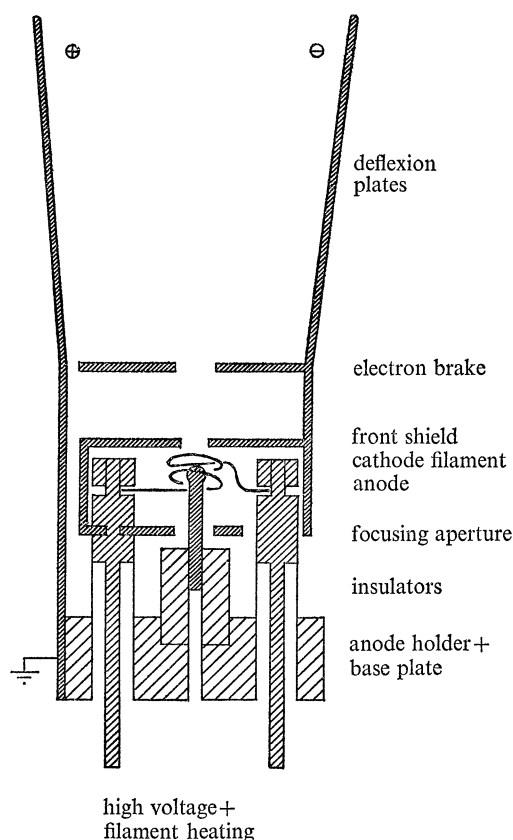


FIGURE 20. Electron gun for shadow casting. The tip of the anode is bombarded with electrons originating from the cathode filament. The lower end of the rod-shaped anode is cooled by the copper of the anode holder and base plate. The front shield hinders heat radiation from the filament. The electron brake and the deflexion plates prevent electron bombardment of the specimen.

the evaporation on the cold specimen. Up to now, the technique used for Pt-C shadow casting (Moor 1959) has shown best results, but it was not always reproducible and produces a rather coarse replica structure. An improvement of the evaporation technique has been the application of electron bombardment heating. Such electron guns are able to evaporate highest melting-point metals which are supposed to create extremely fine-grained high-resolving films.

Conventional guns emit intensive radiation which warms up the fracture face (figures 18 and 19, plate 21). Heat is transferred to the specimen by radiation from the heavy metal source and from the cathode filament of the gun, by condensation of the evaporated material and by electron bombardment. Condensation heating can be neglected if the film is formed slowly (in more than 5 to 10 s). Radiation from the heated heavy metal has to be reduced by the

application of a small source (3 mm²) and a large distance between gun and specimen (15 cm). Heat radiation from the cathode filament can be eliminated with the front shield of the gun; electron bombardment of the specimen is excluded by the application of an additional aperture (electron brake) and two deflexion plates, one of which is connected with the cathode the other with the anode (figure 20).

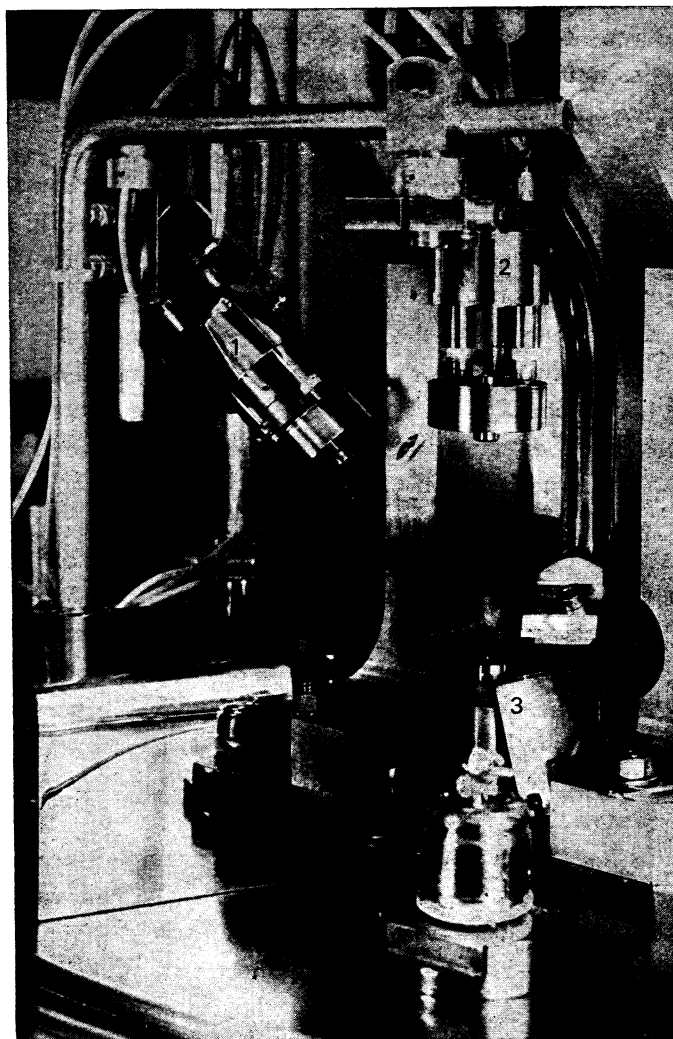


FIGURE 21. The freeze-etching device equipped with electron guns for the evaporation of heavy metal (1) and pure carbon (2) and a quartz crystal sensor head (3) for thin film measurement. The deflexion plates are removed to show the guns more clearly.

For our experiments we have used a Balzers electron bombardment evaporation unit equipped with a slightly modified gun (figure 21). It is equivalent in principle to the apparatus described by Zingsheim, Abermann & Bachmann (1970). The applied voltage was 2 to 2.5 kV the electron beam current 100 to 150 mA.

This system is relatively limited in application because only W and C can be used as anode material. Other high melting-point metals like Pt, Ir, Mo, Ta and Re do not form a stable drop of molten material at the tip of the rod-shaped anode; instead they tend to melt back to the cooled anode holder before the temperature necessary for evaporation is reached. Therefore,

only pure W and Pt or Ta from the tip of a W anode can be evaporated—or pure C and Pt or Ir from a C anode. Only Ta–W, Pt–C and Ir–C produce very fine-grained films which are resistant against the agents used for replica cleaning.

X-ray analysis in an electron microprobe has allowed us to determine the composition of these films. For each sample the same amount of material ($20 \mu\text{g cm}^{-2}$) has been evaporated on a glass coverslip. The mass thickness has been determined by means of a Balzers quartz crystal thin film measurement device (accuracy of $0.1 \mu\text{g cm}^{-2}$). As distance between anode and specimen we have chosen 82 mm. With this arrangement the same amount of evaporated material is needed on the one hand for X-ray analysis samples and on the other hand for shadow casting of specimens which are exposed under an angle of 30° and at a distance of 150 mm. The mass thickness on the shadowed specimens amounts to $3 \mu\text{g cm}^2$. The average thickness of these films cannot be calculated because the density of the alloys is unknown. For calibration purposes samples of pure Pt, Ir, Ta and W have also been measured; pure C did not yield useful counts.

The results of the X-ray analysis are the following: Pt–C contains 5% C, Ir–C 45% C and Ta–W 20% W. Pt–C is a very reproducible system, but it produces relatively grainy films. Ir–C contains too much C for sufficient contrast in the electron microscope. Ta–W produces very fine-grained films, but the system is not stable because from one evaporation to the next the mixture becomes poorer in Ta. From the first to the second evaporation the content of Ta drops from 80 to 65% and reaches 50% at the fifth.

For comparative studies only Ta–W and Pt–C shadow casting can be applied. As a test specimen we have used preparations of polyheads produced by a T4 phage mutant. The regular arrangement of the capsomeres allows the application of optical diffraction methods for image analysis. The polyheads are dried down from aqueous suspension onto Formvar covered gold disks. After shadow-casting the specimens are reinforced by the evaporation of a thin carbon film. By immersion in water the Formvar film and the coated specimen are stripped from the support. After cleaning on nitric acid the polyhead replicas are mounted on specimen grids for electron microscopic observation.

The following results have been obtained: at a support temperature of 20°C Ta–W produces a nearly grainless film (figure 23, plate 22) while Pt–C coating is rather coarse (figure 22, plate 22). Optical diffraction analysis however has demonstrated that the Pt–C film contains much more information than Ta–W (figures 24 and 25, plate 22). This unexpected phenomenon points to the advantage of a limited crystallization of the heavy metal (which causes the graininess). The fine structures of the specimen may act as nuclei for crystallization and in this way structural details are accentuated and can be recorded. Therefore, we have to conclude that a reduction of the grain size of evaporated films by the use of the highest melting-point metals does not necessarily increase the amount of structural information obtained.

The directly visible information of a Pt–C replica can be greatly improved by shadow casting specimens cooled to very low temperatures. Polyhead preparations have been processed as described above but cooled to -150°C in a water free high vacuum of 10^{-6} N m^{-2} (10^{-8} Torr). The Pt–C films obtained this way are not completely free of crystallization, but they show the highest resolution obtained up to now (figure 26, plate 22).

Therefore, it is supposed that the maximum information from the shadow casting technique can be obtained by establishing the optimum granularity level for a given specimen, rather than by merely reducing the granularity to a minimum. The action of fine structures of the

specimen in providing nuclei for crystallization (i.e. a 'decoration effect') may help greatly in revealing structural details of the specimen.

The author wishes to express his thanks to Mr H. Waldner for technical assistance, to Mr W. Hauenstein for the production of double replicas, to Mr R. Gubser (Institute of Crystallography, E.T.H., Zürich) for X-ray analysis, to Dr D. Scraba (University of Geneva) for preparation of polyheads and optical diffraction analysis, to Miss C. Berger for the production of freeze etchings, to Miss S. Türler for drawings and Professor M. Neushul (University of California) for help with the manuscript.

REFERENCES (Moor)

- Bridgman, P. W. 1912 *Proc. Am. Acad.* **47**, 441-558.
 Höchli, M. 1969 unpublished (Diplomarbeit, ETH).
 Moor, H. 1959 *J. Ultrastruc. Res.* **2**, 393-422.
 Moor, H. 1964 *Z. Zellforsch.* **62**, 546-580.
 Moor, H. 1966a *Int. Rev. exptl Path.* **5**, 179-216.
 Moor, H. 1966b Balzers high vacuum report **9**, 1-12.
 Moor, H. 1967 *Protoplasma* **64**, 89-103.
 Moor, H. & Riehle, U. 1968 *Proc. 4th Europ. Reg. Conf. Electron Micr.* **2**, 33-34.
 Pinto, P. & Branton, D. 1970 (in the Press.)
 Riehle, U. 1968 Dissertation ETH, no. 4271, Zürich.
 Staehelin, A. & Bertaud, W. S. 1969 *27th An. Proc. EMSA*.
 Steere, R. L. & Moseley, M. 1969 *27th An. Proc. EMSA*.
 Wecke, J. 1968 Inaugural-Dissertation, Freie Universität Berlin.
 Wehrli, E., Mühlethaler, K. & Moor, H. 1970 *Exptl Cell Res.* **59**, 336-339.
 Weinstein, R. S. 1969 in *Red cell membrane structure and function*, pp. 36-76 (ed. Jamieson & Greenwalt). Philadelphia: Lippincott Comp.
 Zingsheim, H. P., Abermann, R. & Bachmann, L. 1970 *J. Phys. E*, **3**, 39-42.

Downloaded from rstb.royalsocietypublishing.org

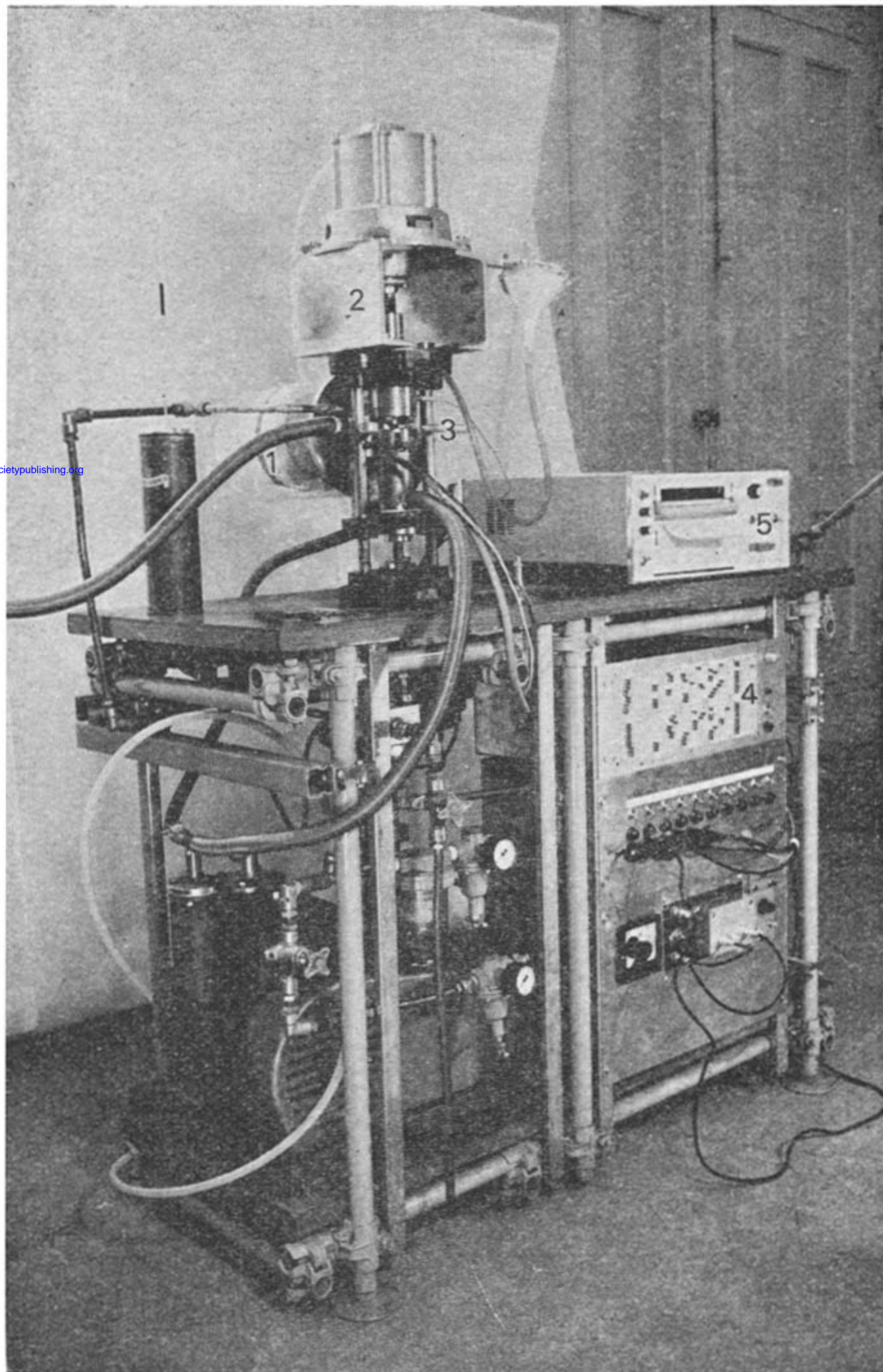
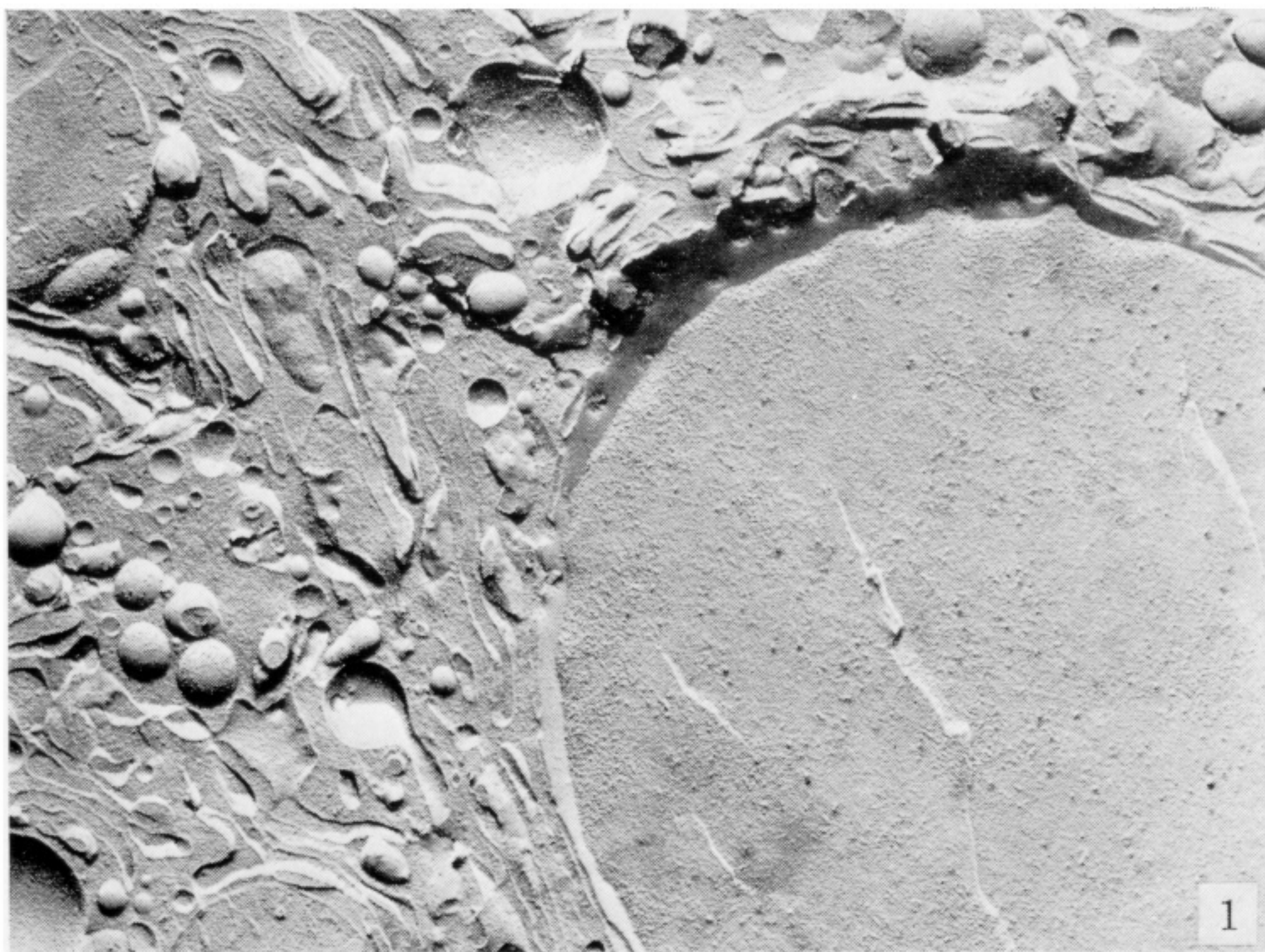


FIGURE 3. The apparatus used for snap-freezing under high pressure. 1, nitrogen supply; 2, pressure supply; 3, specimen stage; 4, time relay for automatic processing; 5, u.v. recorder of temperature and pressure in the specimen stage.



Downloaded from rstb.royalsocietypublishing.org

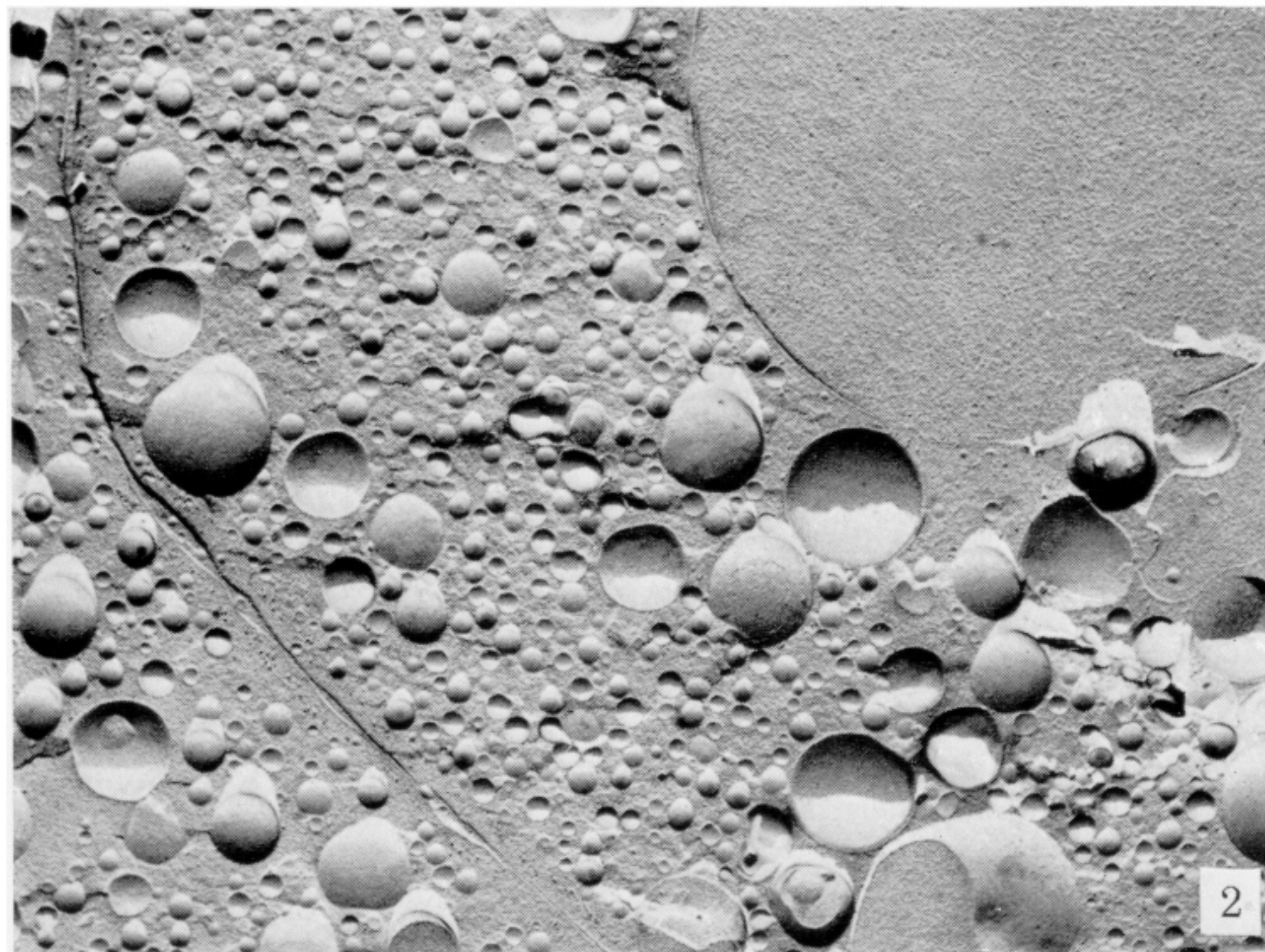
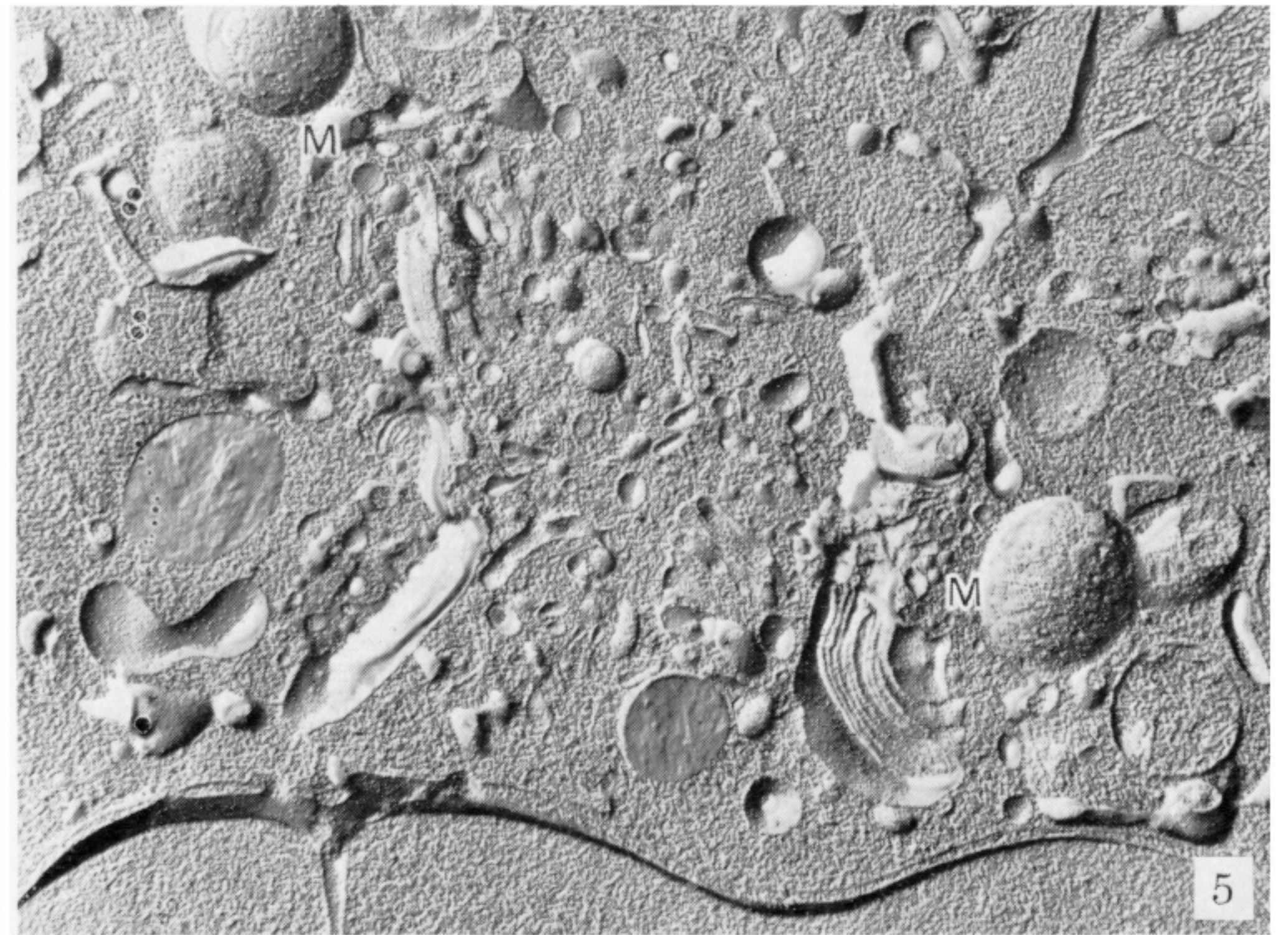


FIGURE 1. A liver cell, prefixed with glutaraldehyde, impregnated with 30% glycerol and freeze-etched, shows a laminar e.r. system. (Magn. $\times 12000$.)

FIGURE 2. The same specimen, treated with 30% glycerol in the living state exhibits a vesiculated e.r. system. (Magn. $\times 12000$.)

FIGURE 5. Part of an ascites tumour cell, protected with 30% glycerol and freeze-etched in the usual way. (Magn. $\times 19200$.)

FIGURE 6. The same type of specimen freeze-fixed under high pressure without antifreeze protection. The same quality of vitrification is obtainable with either antifreeze agents or high pressure freezing. (Magn. $\times 12800$.) The glycerol treatment produces spherical mitochondria (M), the pressure freezing rod-shaped organelles.



Downloaded from rstb.royalsocietypublishing.org



FIGURES 10, 11. Double replica of the plasmalemma of baker's yeast. The two complementary figures can be brought into juxtaposition by folding along the axis between the two photographs. In figure 10 we are looking from the cell wall side, in figure 11 from the cytoplasmic side at the fracture face. (Magn. $\times 48000$.)

FIGURE 12. Heavy contamination on a yeast plasmalemma at $-150\text{ }^{\circ}\text{C}$ exposed to a conventional vacuum of 10^{-4} N m^{-2} Torr). (Magn. $\times 92000$.)

FIGURE 13. A non-contaminated yeast plasmalemma at $-150\text{ }^{\circ}\text{C}$ exposed to a cleansed vacuum of 10^{-5} N m^{-2} (10^{-7} Torr). (Magn. $\times 92000$.)

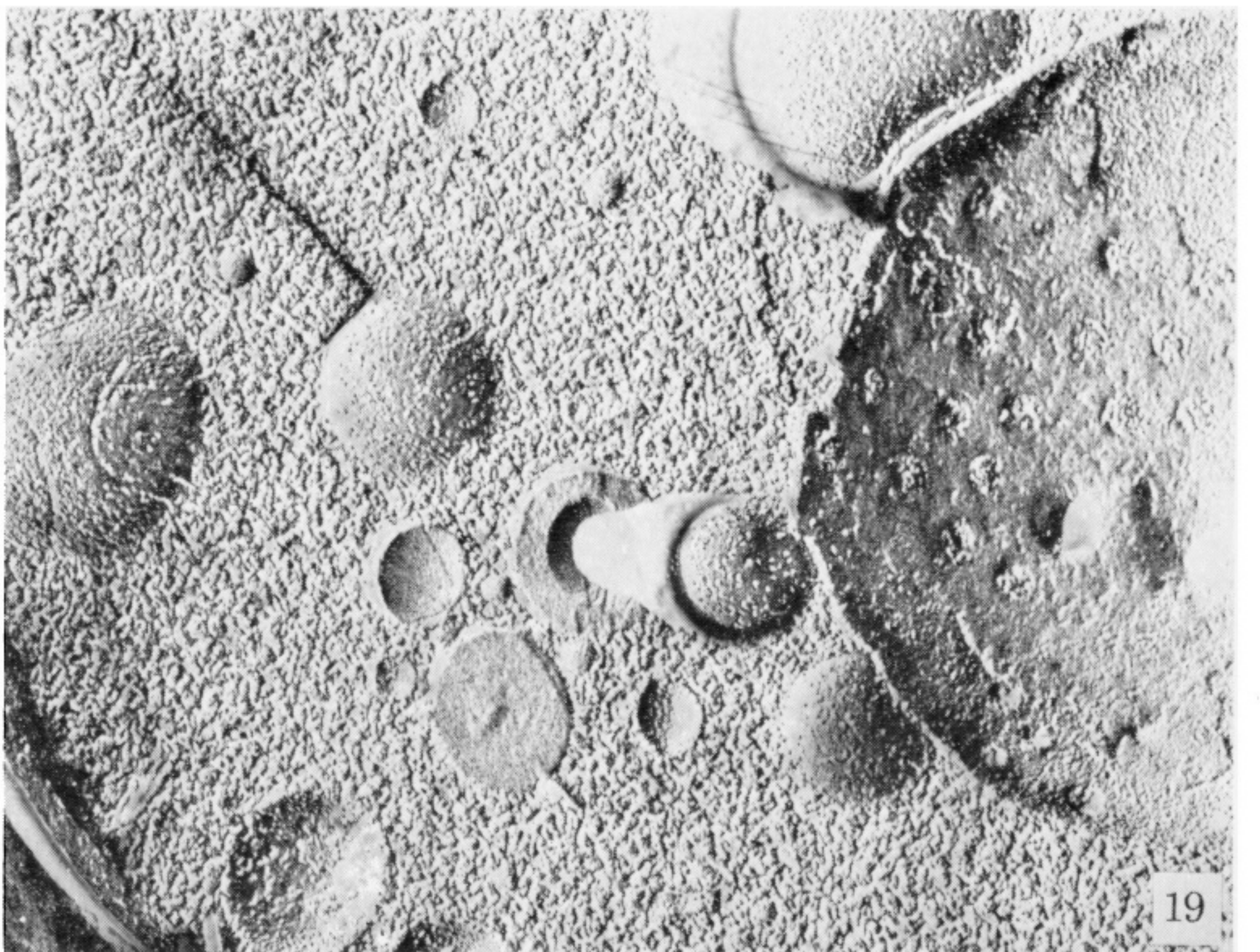
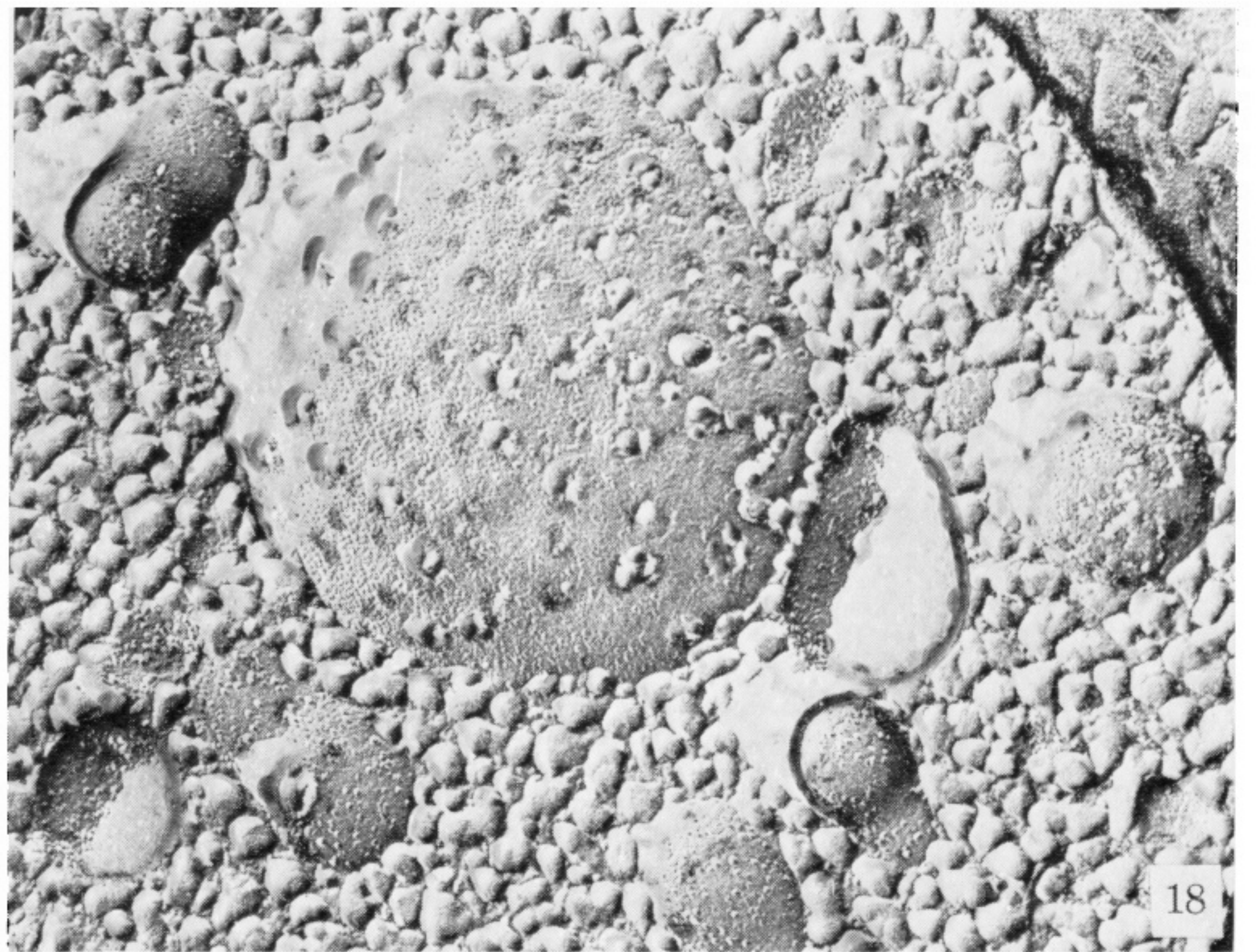
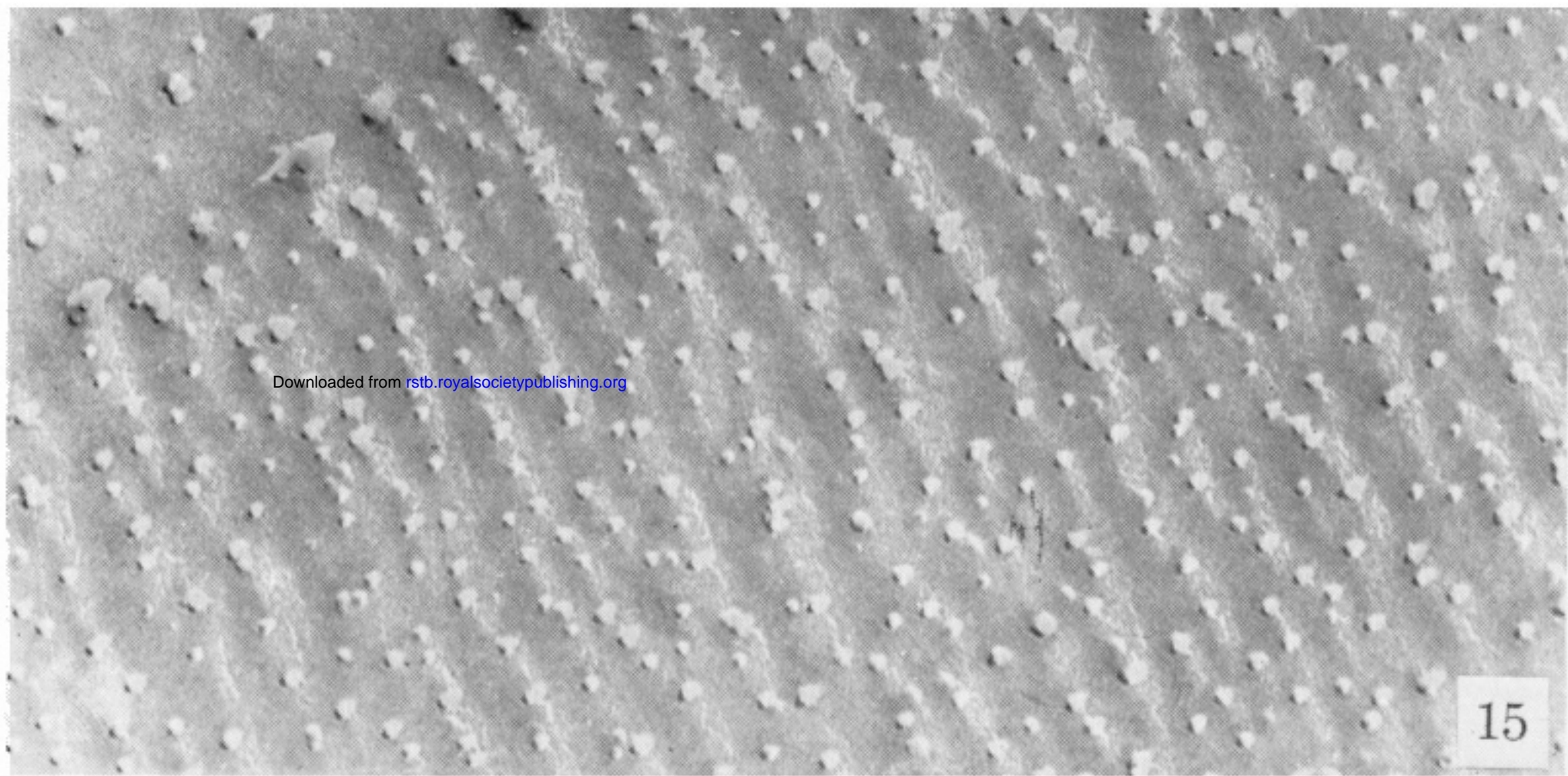
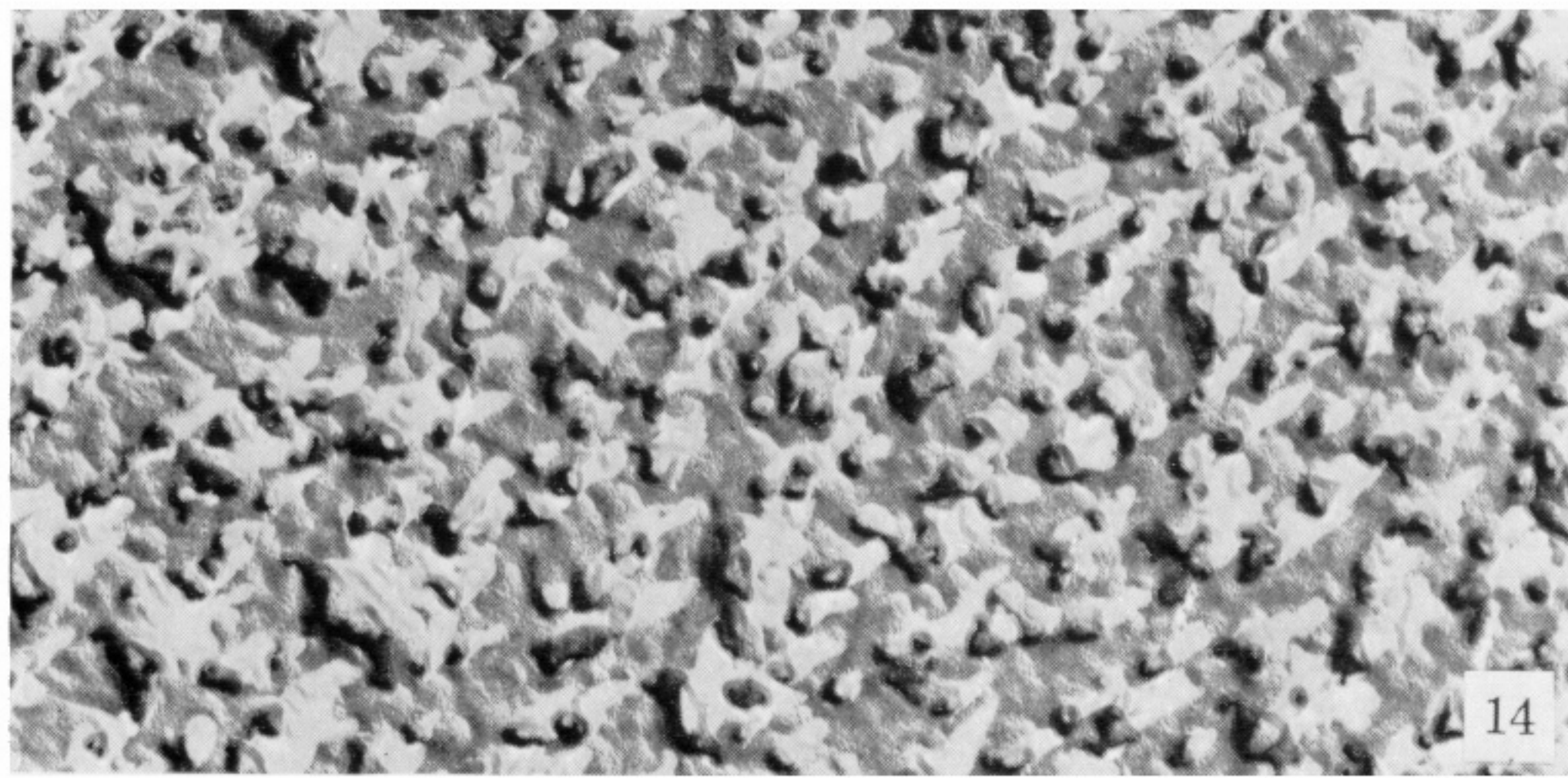


FIGURE 14. An etched ice surface at $-100\text{ }^{\circ}\text{C}$ exposed to a conventional vacuum of 10^{-4} N m^{-2} (10^{-6} Torr). (Magn. $\times 48\,000$.)

FIGURE 15. The same specimen exposed to a cleaned vacuum of 10^{-5} N m^{-2} (10^{-7} Torr). (Magn. $\times 48\,000$.)

FIGURE 16. The same specimen exposed to an ultrahigh vacuum of 10^{-6} N m^{-2} (10^{-8} Torr). (Magn. $\times 56\,000$.)

FIGURE 18. Freeze-etched cell of baker's yeast destroyed by heat radiation. (Magn. $\times 32\,000$.)

FIGURE 19. An area of the same specimen without destruction. (Magn. $\times 32\,000$.)

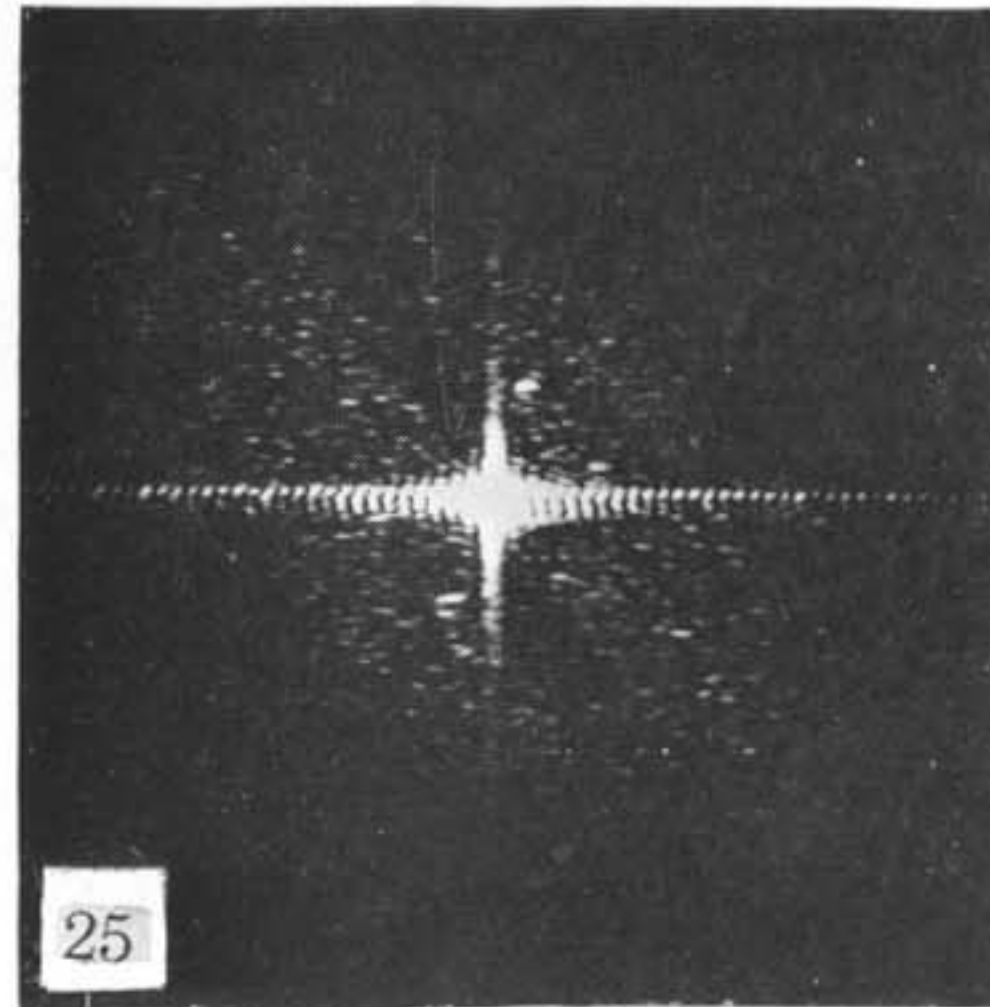
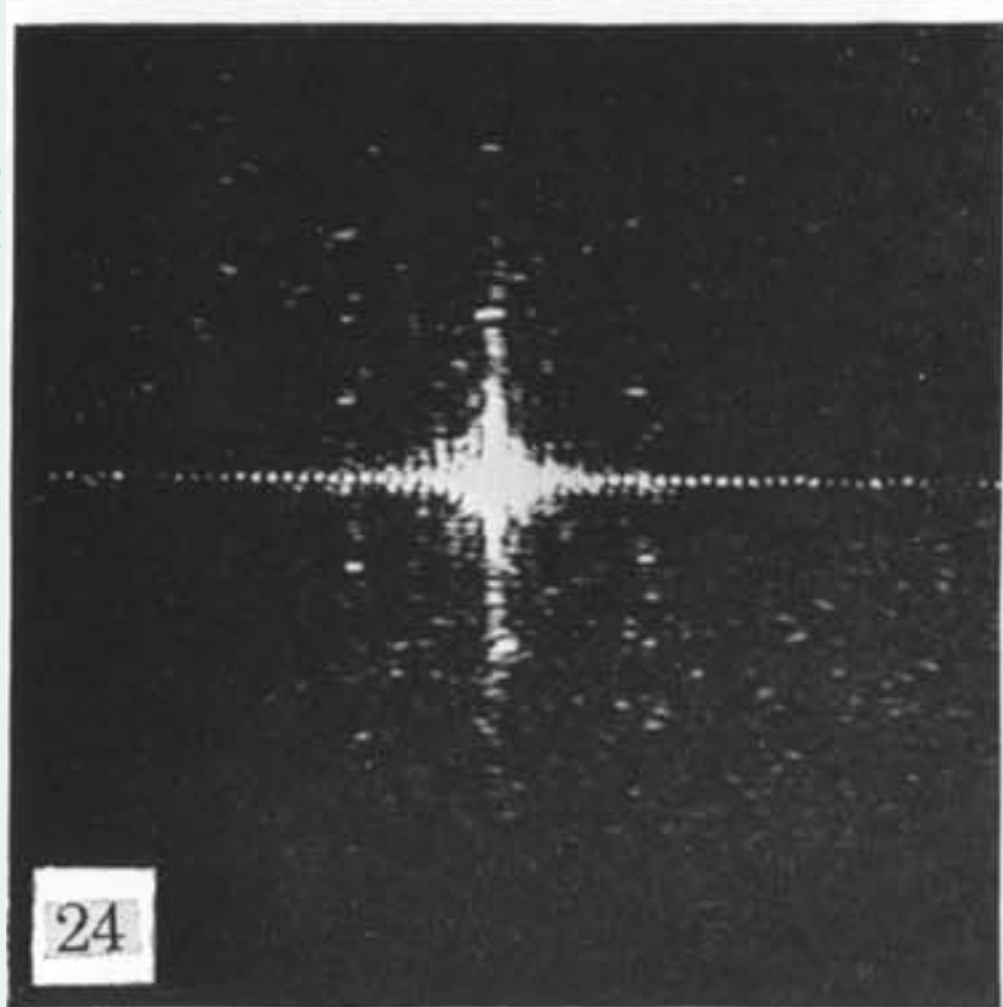
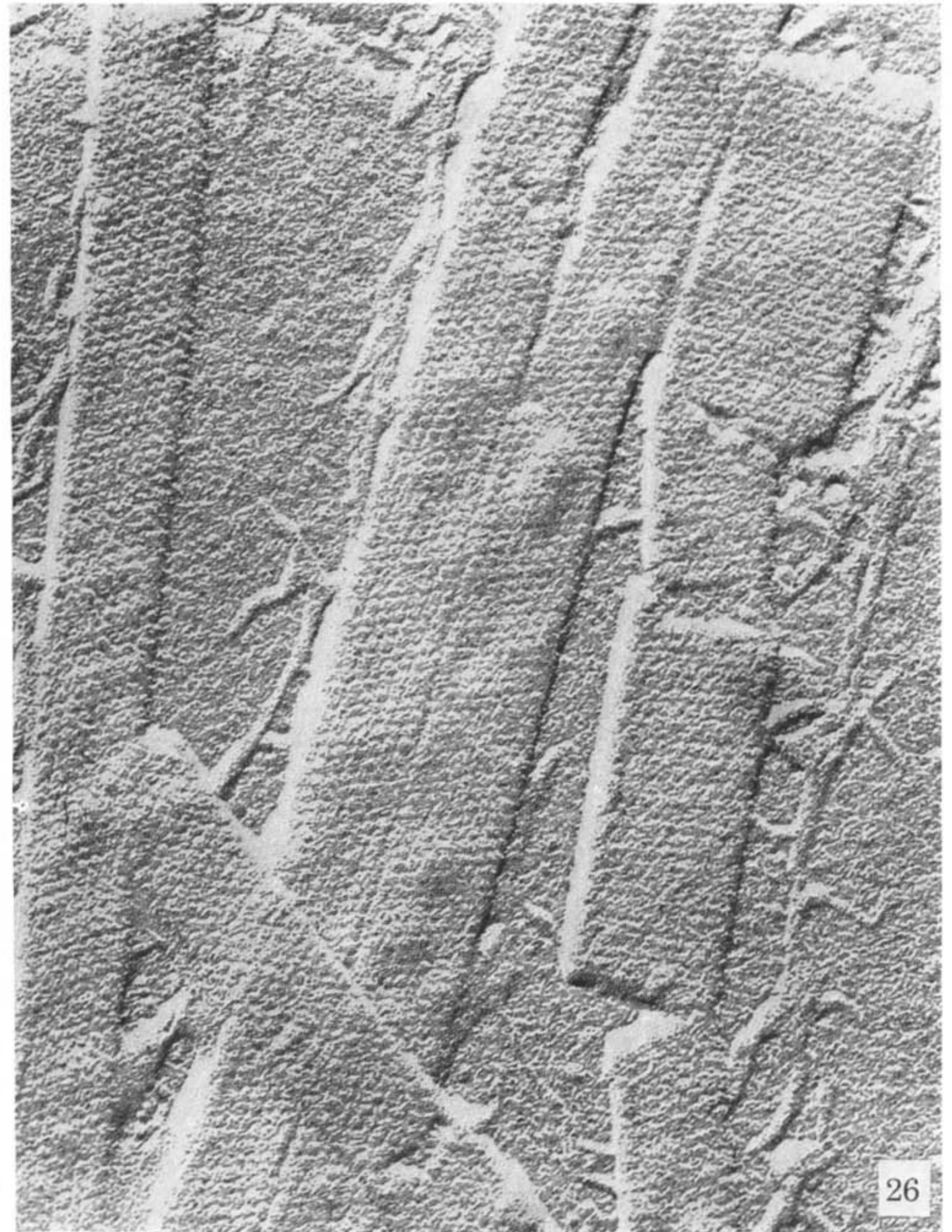
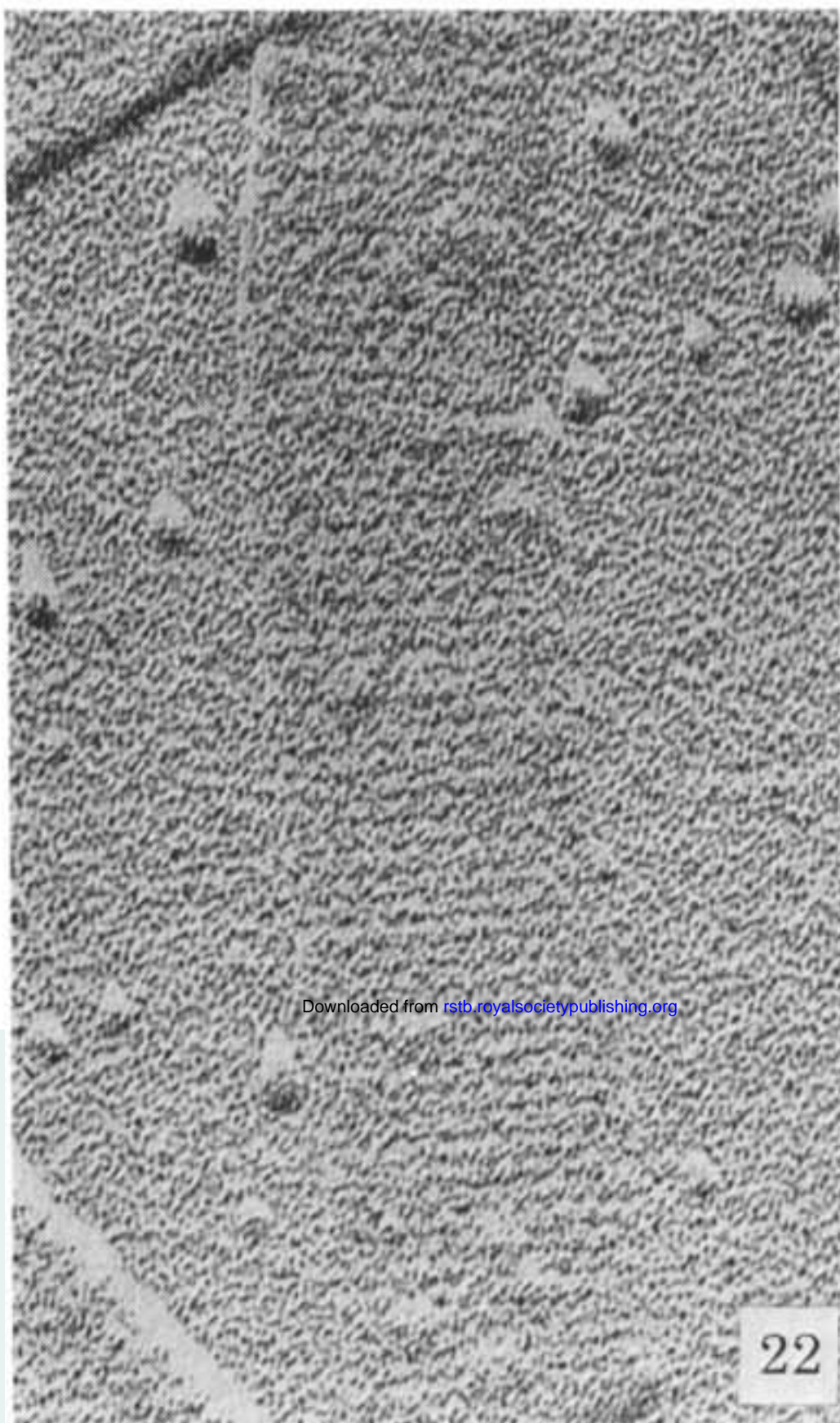


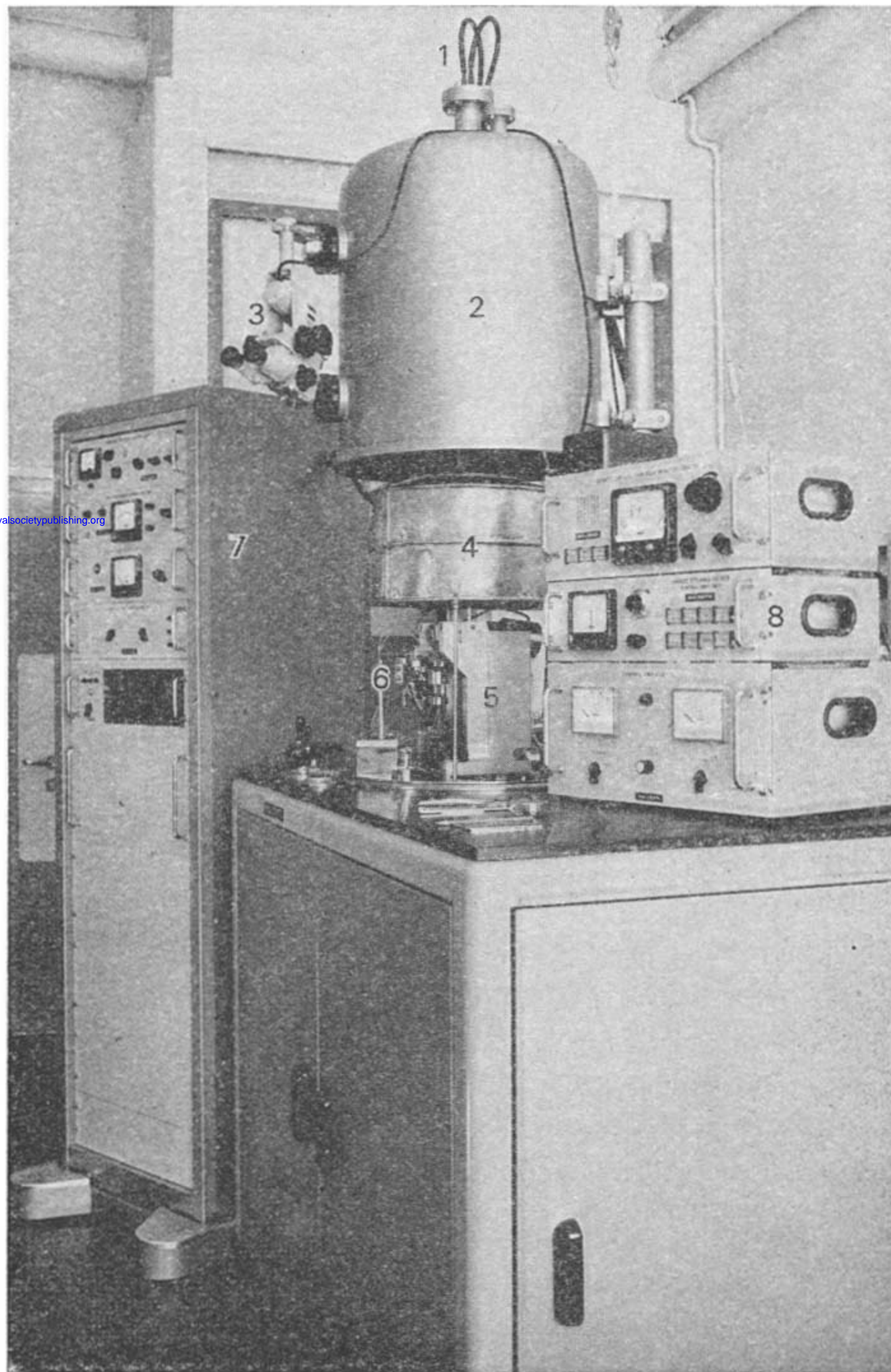
FIGURE 22. Polyhead preparation at 20 °C shadowed with Pt-C. Substructures of the capsomeres can be made visible only by optical diffraction. (Magn. $\times 132000$.)

FIGURE 23. Polyhead preparation at 20 °C shadowed with Ta-W. Substructures of the capsomeres are not visible. (Magn. $\times 132000$.)

FIGURE 24. Optical diffraction of figure 22.

FIGURE 25. Optical diffraction of figure 23.

FIGURE 26. Polyhead preparation at -150 °C shadowed with Pt-C. Substructures of the capsomeres are directly visible. (Magn. $\times 132000$.)



Downloaded from rstb.royalsocietypublishing.org

FIGURE 17. The Balzers high vacuum plant BA 510 A used for freeze-etching: 1, Ti-sublimation pump; 2, bell jar; 3, binocular microscope for specimen observation; 4, the additional large cold trap; 5, microtome; 6, electron guns, 7, vacuum control units, 8, control units for thin film measurement, freeze-etching and evaporations.

Downloaded from rstb.royalsocietypublishing.org

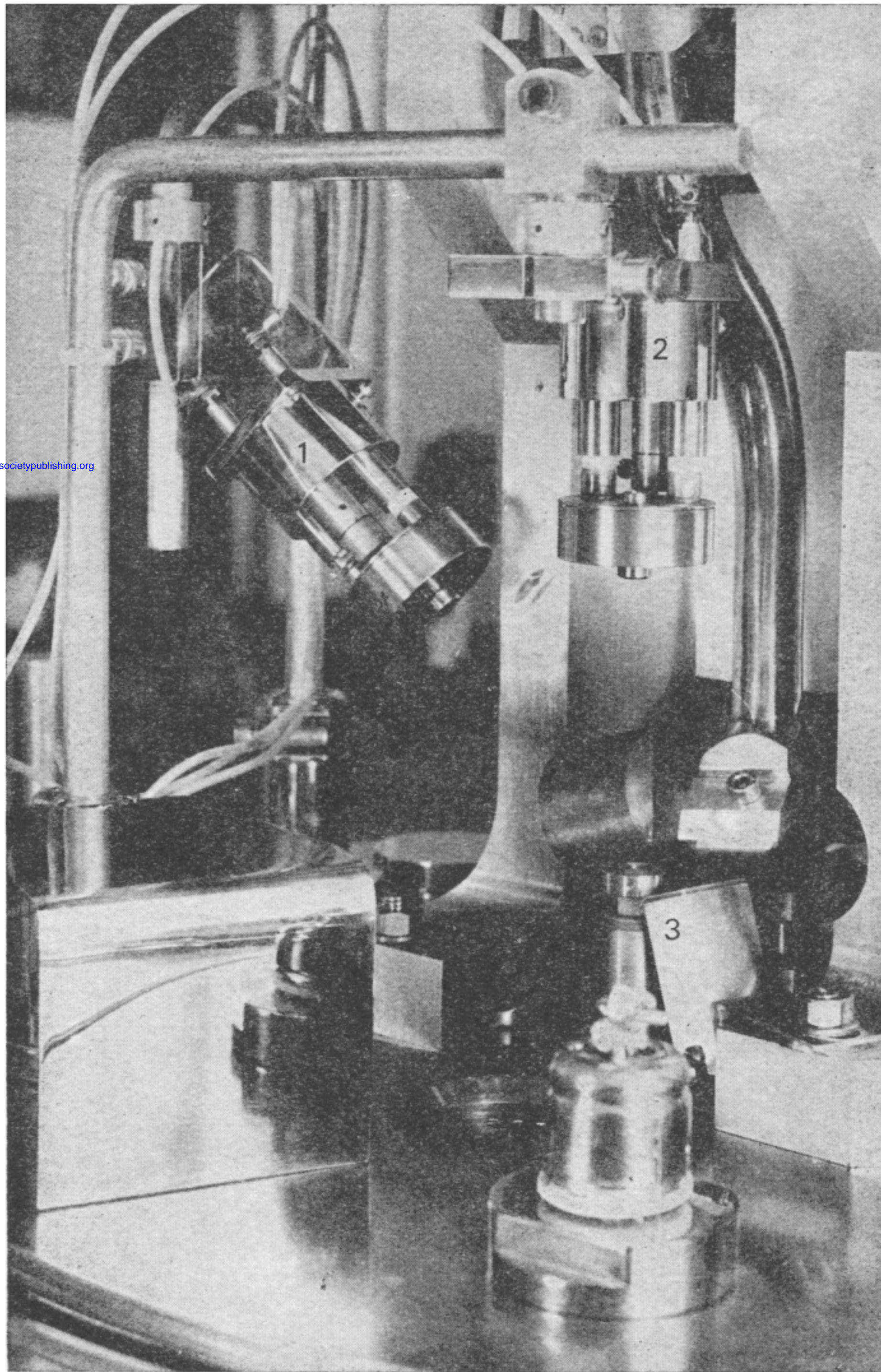


FIGURE 21. The freeze-etching device equipped with electron guns for the evaporation of heavy metal (1) and pure carbon (2) and a quartz crystal sensor head (3) for thin film measurement. The deflexion plates are removed to show the guns more clearly.